



Delta Journal of Science  
Available online at <https://djs.journals.ekb.eg/>



Research Article

**GEOLOGY**

## Conventional and Advanced Petrophysical Evaluation of Pliocene Sediments, Simian Field, Offshore West Nile Delta Basin, Egypt

Hassan El-Kadi<sup>1</sup>, Mohamed Musaad<sup>1</sup> and Ashraf El-Sayed<sup>1</sup>

<sup>1</sup>Geology Department, Faculty of Science, Al-Azhar University, Egypt

Corresponding author: Ashraf El-Sayed

e-mail: [geoasm2020@gmail.com](mailto:geoasm2020@gmail.com)

Received: 5/2/2022

Accepted: 13 /6/2022

### KEY WORD/S/

### ABSTRACT

Nile Delt Basin:

El-Wastani  
Formation:

Petrophysical  
Interpretation:

The study area is located approximately 120km NE of Alexandria, which lies offshore in the deep water (250-1500m) of the Nile Delta and bordered between latitudes 32° 16` & 32° 06`N and longitudes 30° 44` & 30° 56`E. Simian element is one of the major channel systems that make up the Mid- Pliocene submarine channel complex as mapped in the West Delta Deep marine concession. The materials used in this study include collection and description of the complete log sets from four wells in the study area, including the conventional logs; Gamma Ray (GR), Caliper, Deep and Shallow Laterolog resistivities (LLD, LLS), Micro-Spherically Focused log (MSFL), and porosity tools (Density, Neutron, and Sonic), also the advanced logs; Formation Micro Image (FMI), Combinable Magnetic Resonance (CMR), and Modular Dynamic Tester (MDT). The petrophysical interpretation showed that the effective porosity ranges from 21% to 25% and the water saturation ranges from 29% to 40%, and the volume of shale is from 16% to 29%. Generally, the distribution of the petrophysical parameters increase from the core of the channel toward its levee along the channel axis of the study area. The optimum location for the proposed wells is the southeastern parts of the field, where the lower shale volume and net to gross, and the higher porosity and hydrocarbon saturation values are of the combination of structural amplitude map and petrophysical maps the best drilling for future consideration helped to locate new locations.

## 1. Introduction

The Simian field is located at the northwestern margin of the Nile Delta, approximately 120 km offshore of Alexandria. The field lies in the West Delta Deep Marine Concession (Fig. 1). It lies at the cross of Lat 32° 10' 48.085" N and long 30° 49' 21.733" E. Simian element is one of the major channel systems that make up the Mid-Pliocene submarine channel complex mapped in the West Delta Deep Marine Concession area (Beshry, 2014).

El Wastani Formation consists of thick sand beds interbedded with thin clay levels which become thinner toward the top of the formation. The depositional environment of this formation is transitional between the shelf facies of Kafr El Sheikh Formation and coastal or shallow marine to fluvio-marine sands of the overlying Mit Ghamr Formation (Shehab, 2018). This

formation was deposited during the late Pliocene time, in which the sea regression started to close the sedimentation cycle of the Pliocene, which began by the sea transgression of the Abu Madi Formation. The type of section is at El Wastani-1 well with thickness (394 ft).

4 wells in Simian field are chosen for this study. These are Simian-1, 2 (Dj), 3 (Dh), and Dp) (Fig.1). The first was Simian-1, which proved a good quality channel facies in the upper slope Simian channel, and penetrated the base channel filled with gravel (British Gas (BG), 1999).

Simian channel lies at the base of the El Wastani Formation, at a similar level to the many slope channels laying in the same play in the offshore Nile Delta area (Beshry, 2014).

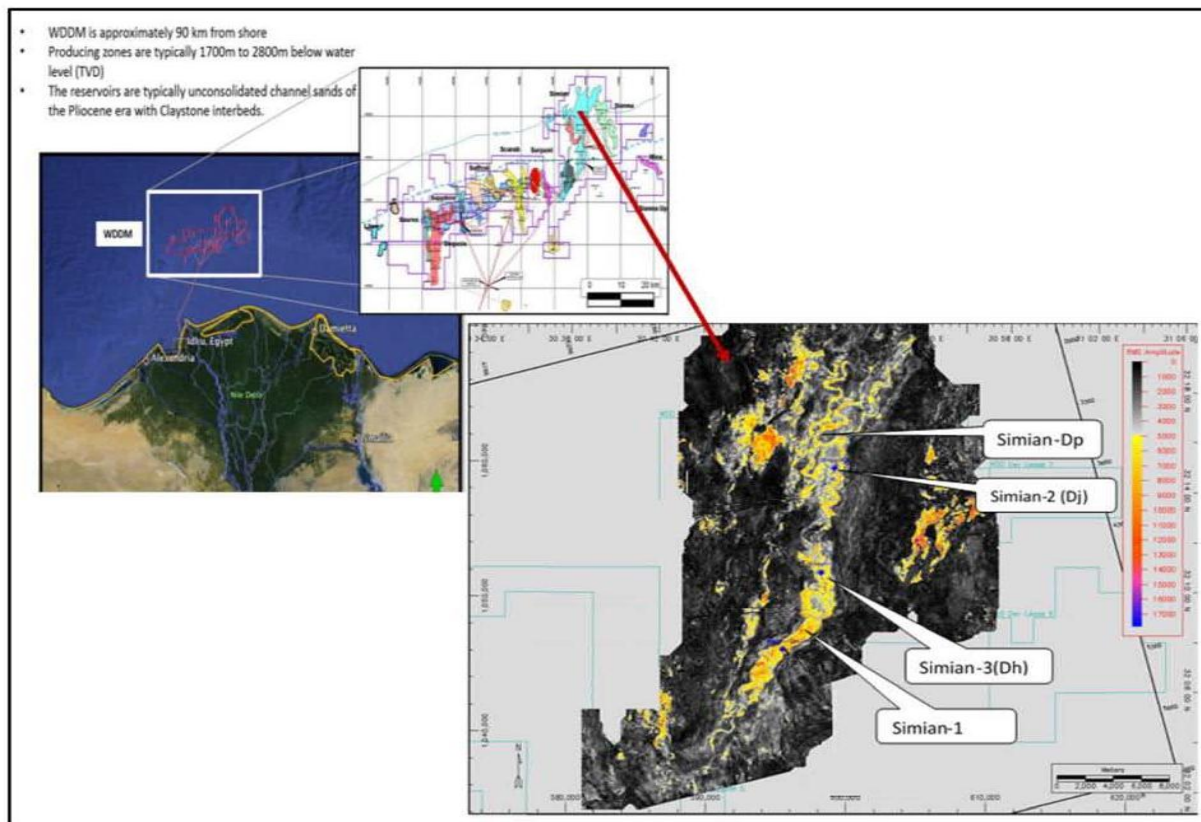


**Fig. 1:** Satellite view of Nile Delta contain Simian Field and location of wells chosen for this Study

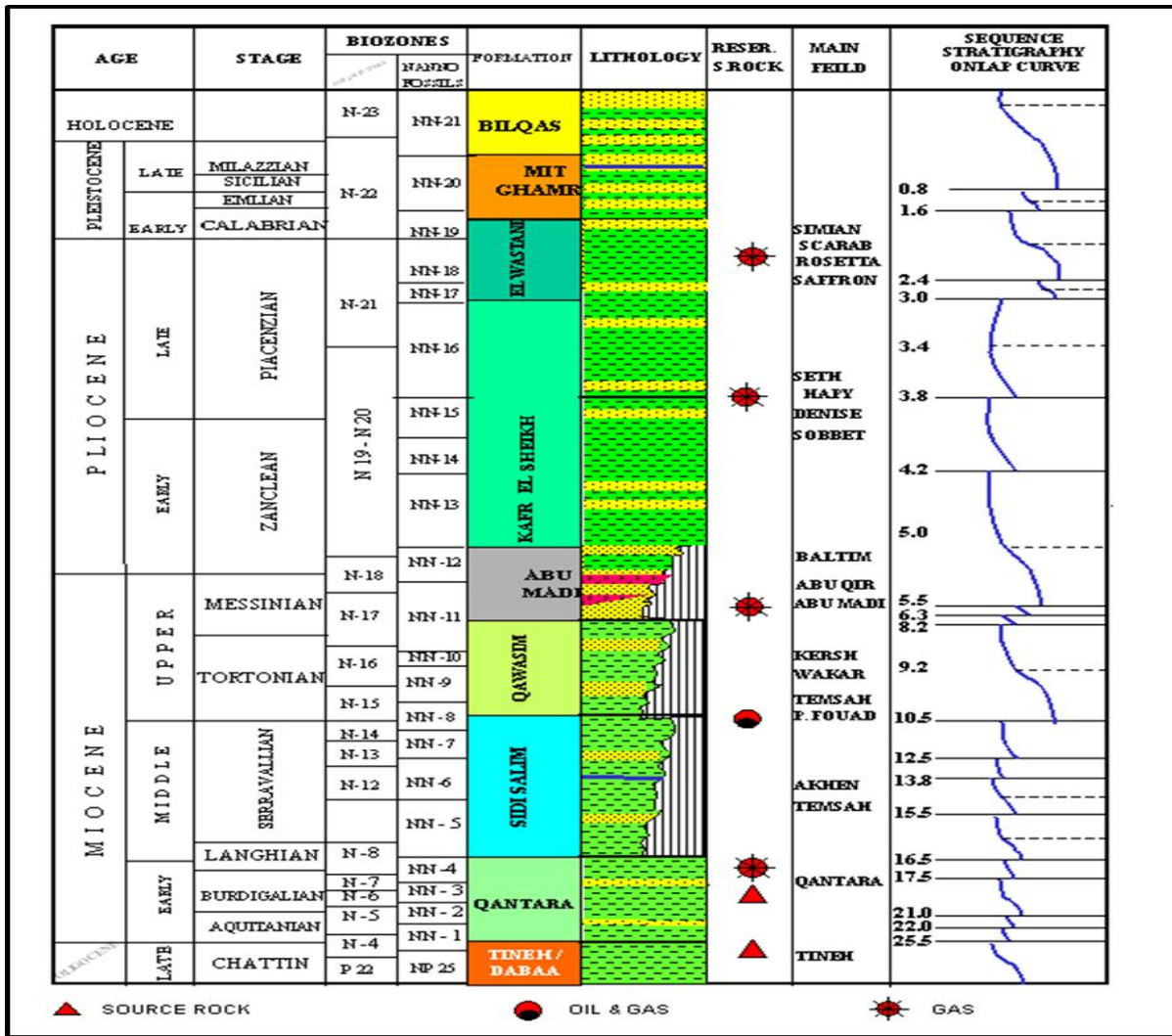


Fig. 2. Generalized lithostratigraphic column of the Simian Field

## 2. Formation Evaluation Methodology

A comprehensive analytical formation evaluation system is established to interpret the basic and advanced logging data for the deduction of the petrophysical parameters of the analysed units based on a number of equations and empirical relations, as well as charts using Techlog program.

### 2.1. Conventional Formation Evaluation Technique

A) Clay content from conventional tools:  
The volume of shale is calculated from gamma ray (Schlumberger, 2004) as follow:

$$V_{sh} = \frac{GR - GR_{min}}{GR_{max} - GR_{min}} \quad (1) \text{ Schlumberger, 2004}$$

Where:

- GR: is the gamma ray reading
- GR min: is the gamma ray of clean sand
- GR max: is the gamma ray of clay

B) Porosity from conventional tools:  
The porosity is calculated from the density and neutron method using the following equation (Wyllie, 1963):

$$\phi_d = \frac{\rho_{mat} - \rho_b - V_{sh} * (\rho_{mat} - \rho_{sh})}{\rho_{mat} - \rho_{fluid}} \quad \dots(2) \text{ Wyllie, 1963}$$

$$\phi_{Nc} = (\phi_N - \phi_{Nsh} V_{sh}) \quad \dots(3) \text{ Dewan, 1983}$$

Combining data from the neutron and density logs. Porosities can be calculated through the following equations (Schlumberger, 1987):

$$\Phi = (\Phi_D + \Phi_N) / 2 \dots (4) \text{ Schlumberger, 1987}$$

C) Water saturation is estimated using Indonesia equation as follow:

a) Indonesia equation for invaded zones:

$$\frac{1}{(Rt)^{\frac{1}{2}}} = (S_w)^{\frac{n}{2}} * \left[ \left( \frac{Vsh^{(1 - \frac{Vsh}{2})}}{Rsh^{\frac{1}{2}}} \right) + \left( \frac{\phi^m}{(a R_w)^{\frac{1}{2}}} \right) \right]$$

..... (5) Schlumberger, 1972

b) Indonesia equation for noninvaded zones (Schlumberger, 1972):

$$\frac{1}{(Rxo)^{\frac{1}{2}}} = (Sxo)^{\frac{n}{2}} * \left[ \left( \frac{Vsh^{(1 - \frac{Vsh}{2})}}{Rsh^{\frac{1}{2}}} \right) + \left( \frac{\phi^m}{(a Rmf)^{\frac{1}{2}}} \right) \right]$$

..... (6) Schlumberger, 1972

## 2.2 Advanced Formation Evaluation Technique

A) Corrected Total Porosity from CMR is applied using the following equation:

$$PGAS1 = \frac{(DPHZ * (1 - \frac{HIG * PGA}{HIF})) + (LAMDA * \frac{TCMR}{HIF})}{((1 - \frac{HIG * PGA}{HIF}) + LAMDA)}$$

.....(7) Rashpetco/BG (2005)

DMRP=IF ((DPHZ<TCMR), TCMR, PGAS1)

.....(8) Rashpetco/BG 2005

B) Corrected Effective Porosity from CMR

The Corrected effective porosity from the CMR is calculated from the following relation:

$$CMRP\_3MS = \frac{DMRP - CBF2}{CBF2}$$

.....(9) Rashpetco/BG (2005)

C) Volume of Clay (VCL) by using the CBF2

The volume of shale Vsh can be calculated from the CBF2 as from the following relation:

$$Vsh = \frac{CBF2}{CBF2CL} \dots\dots\dots(10) \text{ Rashpetco/BG (2005)}$$

D) Effective Water Saturation (SWE)

The effective water saturation can be calculated by dividing the capillary water by the effective porosity from CMR as from the following relation:

$$SWE = \frac{CIV}{CMRP_{3MS}} \dots\dots\dots(11) \text{ Rashpetco/BG (2005)}$$

E) Permeability Calculation from CMR (KTIM)

KTIM is permeability estimated from the Timur-Coates model, units are mD, as from the following two relations:

$$PERMA = 10^4 * ((CMRP_{3MS4}) * (\frac{CMFF}{CIV})^2)$$

.....(12) Coates *et al.*, (1999)

KTIM=IF ((DPHZ < TCMR), KTIM, PERMA)

..... (13) Timur (1968)

F) Permeability Calculation using SDR model

The SDR model works very well in water-saturated zones, in the presence of oil or oil filtrates as follow

$$KSDR = 4 * DMRP^4 * T2LM^2 \dots\dots\dots(14) \text{Kenyon (1997)}$$

KSDR is the permeability estimated from the SDR model and KTIM is the permeability estimated from the Timur-Coates model 1999, their units are millidarcy.

where:

$\Phi_D$ : is the Porosity derived from Density

$\Phi_N$ : is the Porosity from Neutron

$\Phi_s$ : is the Porosity from Sonic

$\Phi_{eff}$ : is the Effective Porosity

$\Phi_T$  : is the Total Porosity

$V_{sh}$ : is the shale Volume

$\rho_{mat}$ : is the Matrix Density

$\Delta t_{mat}$ : is the Matrix sonic

$\rho_{fl}$ : is the Fluid Density

$\Delta t_{fl}$ : is the Fluid Sonic

RT: is the True Resistivity of the formation.

n : is the Saturation Exponent

a : is the Tortuosity Factor

m: is the Cementation Factor

F : is the Formation Resistivity factor

$R_w$ : is the Water Resistivity, Ohm-m.

HIG: is the Hydrogen Index of Gas

HIF: is the Hydrogen Index of Fluid

PGA: is the Polarization of Gas

DPOR: is the Porosity from Density

DMRP: is the CMR Corrected Total Porosity

CMRP\_3MS: is the CMR Corrected Effective Porosity

CW: is the Capillary Water Volume

SWI: is the Irreducible Water Saturation

SWE: is the Effective Water Saturation

CMFF: is the Gas Corrected Free Fluid Index

$V_{sh}$ : is the shale Volume from CMR

KTIM: is the CMR Permeability Corrected to Gas Effect

### 3. Results

This study deals with the combination of the basic tools (gamma-ray, density, neutron, and resistivity), and the advanced tools (formation micro image, combinable magnetic resonance, modular dynamic tester and sonic). Basic tools detect conventional reservoirs in good way, but they cannot detect the

unconventional reservoirs, that are sometimes under resolution.

Advanced tools detect both the conventional and unconventional reservoirs. These tools have a very high vertical resolution that reaches one centimeter for the Formation Micro Image (FMI).

#### 3.1. Comparison between Conventional and Advanced Models

The litho-saturation plot illustrates the raw log data in a number of tracks. From left to right, the GR with the caliper log readings and bit size, then the depth track, the next track displays the names of the examined formations, the next tracks are the resistivity log including shallow, medium and deep resistivity, Neutron and Density with fill area as a sand indicator, then two tracks for the CMR data, one for the log amplitude, and second for the fluid volumes. The next track is the Formation Micro Image (FMI) as static and dynamic images, then two tracks to show the permeability from the KTIM and KSDR models, next to that is the sonic data, including the compressional and stoneley slowness. The last two tracks are the calculated net reservoir and the net-pay, from the conventional and advanced methods.

The following are the detailed presentations of the selected cross plots constructed for the evaluated rock units, from Simian-1, Simian-2 Simian-3 and Simian-Dp wells (Figs. 3, 4, 5 and 6).

##### 3.1.1. Petrophysical Analysis of the Simian Channel in Simian-1 Well

Simian-1 well is located on the southern part of the study area in proximal part of the Simian channel (Fig. 1). A litho-saturation plot and data logs are displayed for the interval from 2088.5 to 2198 m. This well was

logged by complete sets of tools down to the total depth of 2265m.

Simian channel in this well has a gross thickness of 78.4m. Top channel is encountered through the depths range from 2088 to 2166.4 m. The litho-saturation plot shows that Simian channel consists of sandstone and shale intercalated with silt (Fig. 3).

### **3.1.2. Petrophysical Analysis of the Simian Channel in Simian-3 Well**

Simian-3 well is located in the central part of the study area (Fig. 1). Litho-saturation plot and data logs are displayed for the interval 2065.5m to 2223 m. This well constitutes top Simian channel. This well was logged by a complete set of tools down to a total depth of 2310m. The gross thickness in Simian-3 well is 108 m. The litho-saturation plot (Fig. 5) shows that, the Simian channel consists of sandstone and shale, intercalated with silt.

### **3.1.3. Petrophysical Analysis of the Simian Channel in Simian-2 and Dp Wells**

The Simian-2 and Simian-Dp wells are located at the northern part of the study area, in the distal area of the Simian channel (Fig. 1). Litho-saturation plots and data logs display the intervals from 2103.5 to 2236.5 m and 2146 to 2350 m, respectively, and constitute the top channel. These wells were logged by complete sets of tools down to a total depth of 2236.5 m and 2350 m, respectively.

The Simian channel in these wells (Simian-2 and Simian-Dp) has a gross thickness of 99 m and 127 m, respectively. The top channel is encountered through the depth ranges from 2103.5m to 2202.5m and from 2146 m to 2273 m, respectively. The litho-saturation plots (Figs. 4 and 6) shows

that Simian channel consists of sandstones, intercalated with shale.

The average petrophysical parameters of conventional and advanced results used in this study include volume of shale, total porosity, effective porosity and fluid saturation (water saturation and hydrocarbon saturation) are tabulated in the following tables (1 and 2).

**Table 1:** Calculated Petrophysical Parameters Using Conventional Model

| Well      | Thickness (m) | Net Pay (m) | Shale Volume% | Effective porosity% | Hydrocarbon Saturation% | Hydrocarbon Pore volume (m <sup>3</sup> ) |
|-----------|---------------|-------------|---------------|---------------------|-------------------------|---|
| Simian-1  | 78.4          | 45.6        | 16            | 22                  | 67                      | 6.72                                      |
| Simian-2  | 99.5          | 22          | 27            | 21                  | 66                      | 3.1                                       |
| Simian-3  | 157.5         | 59.7        | 19            | 24                  | 68                      | 9.75                                      |
| Simian-Dp | 127           | 43          | 21            | 22                  | 71                      | 5.99                                      |

**Table 2:** Calculated Petrophysical Parameters Using Advanced Model

| Well      | Thickness (m) | Net Pay (m) | Shale Volume% | Effective porosity% | Hydrocarbon Saturation% | Hydrocarbon Pore volume (m <sup>3</sup> ) |
|-----------|---------------|-------------|---------------|---------------------|-------------------------|---|
| Simian-1  | 78.4          | 53.5        | 18            | 24                  | 65                      | 8.35                                      |
| Simian-2  | 99.5          | 31.2        | 31            | 23                  | 62                      | 4.42                                      |
| Simian-3  | 157.5         | 72          | 21            | 25                  | 65                      | 11.71                                     |
| Simian-Dp | 127           | 48.3        | 29            | 24                  | 60                      | 6.22                                      |

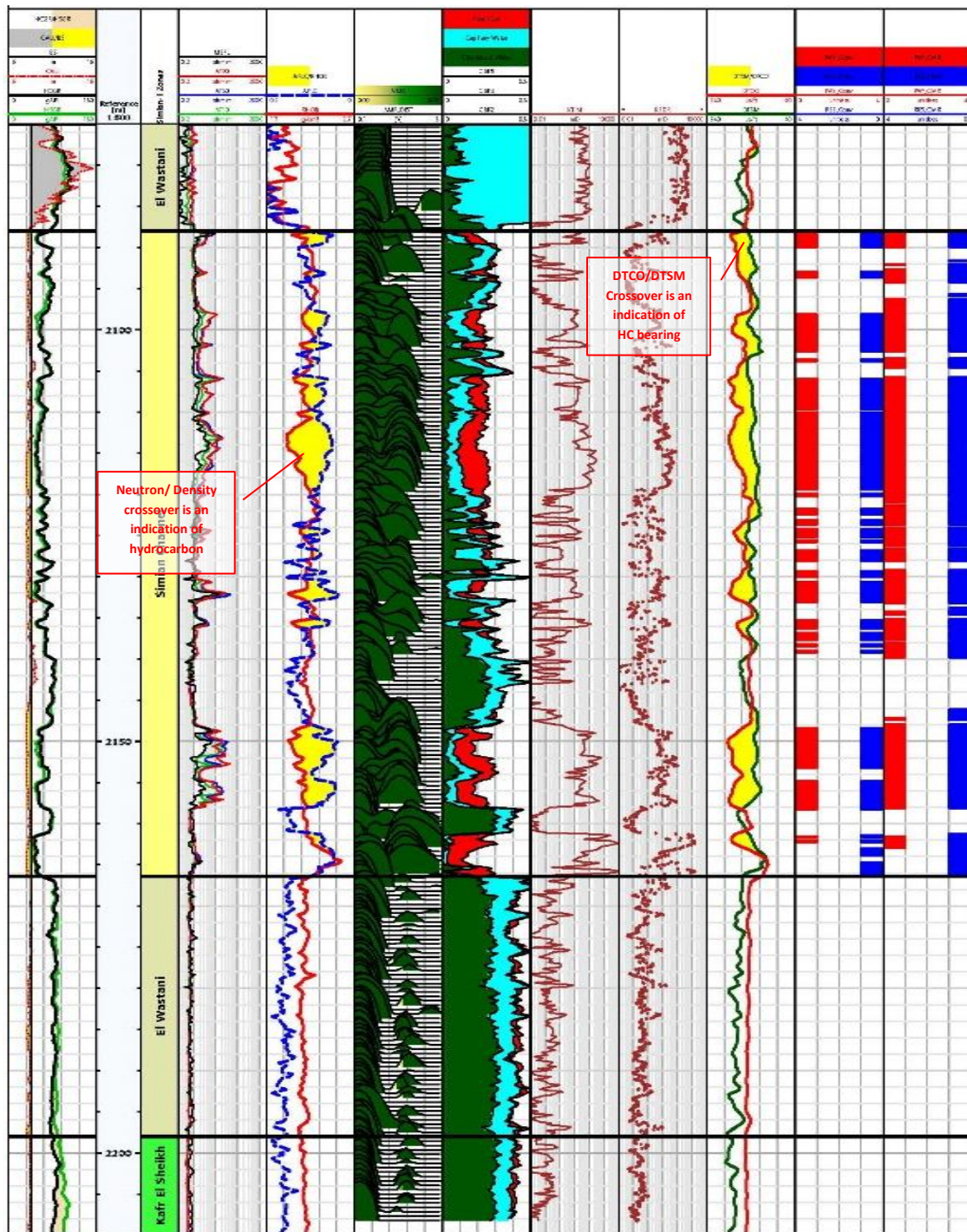


**Fig. 3:** Litho-saturation plot showing integration of basic and advanced logs for detection of conventional and unconventional reservoirs for Simian Channel (El Wastani Formation) in Simian-1 well

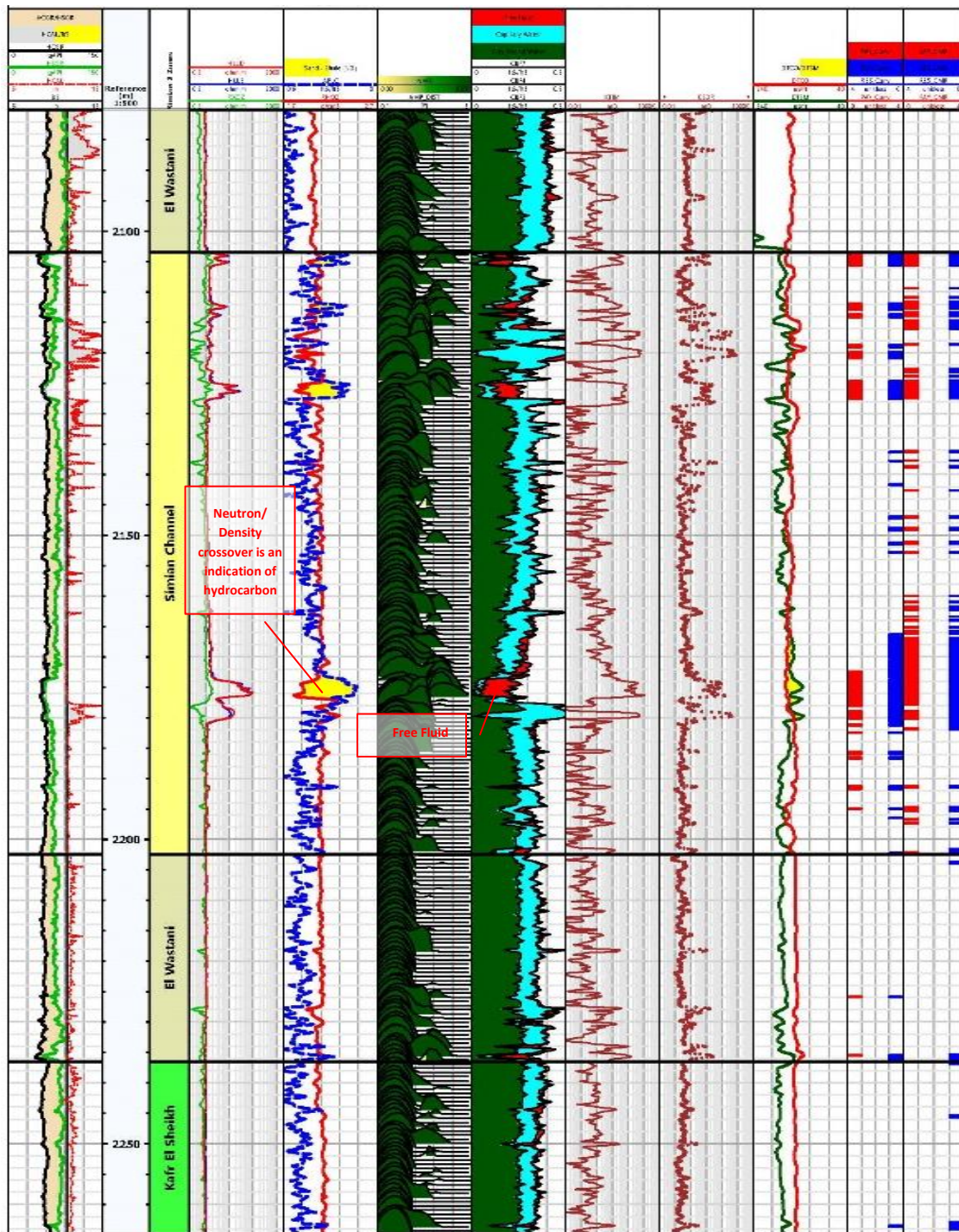


**Fig. 4:** Litho-saturation plot showing integration of basic and advanced logs for detection of conventional and unconventional reservoirs for Simian Channel (El Wastani Formation) in Simian-2 Well

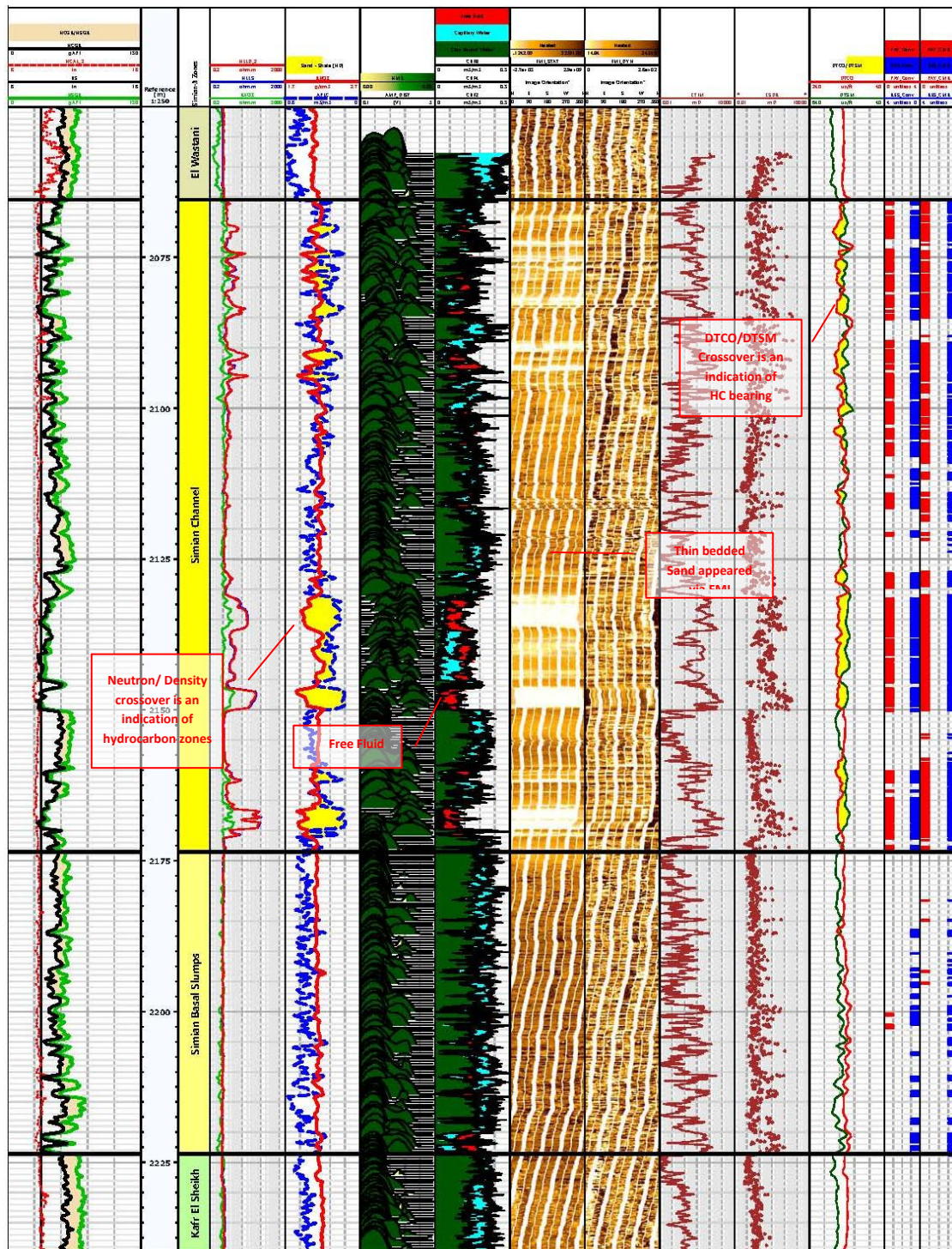


**Fig. 5:** Litho-saturation plot showing integration of basic and advanced logs for detection of conventional and unconventional reservoirs for Simian Channel and Simian Slumps (El Wastani Formation) in Simian-3 Well

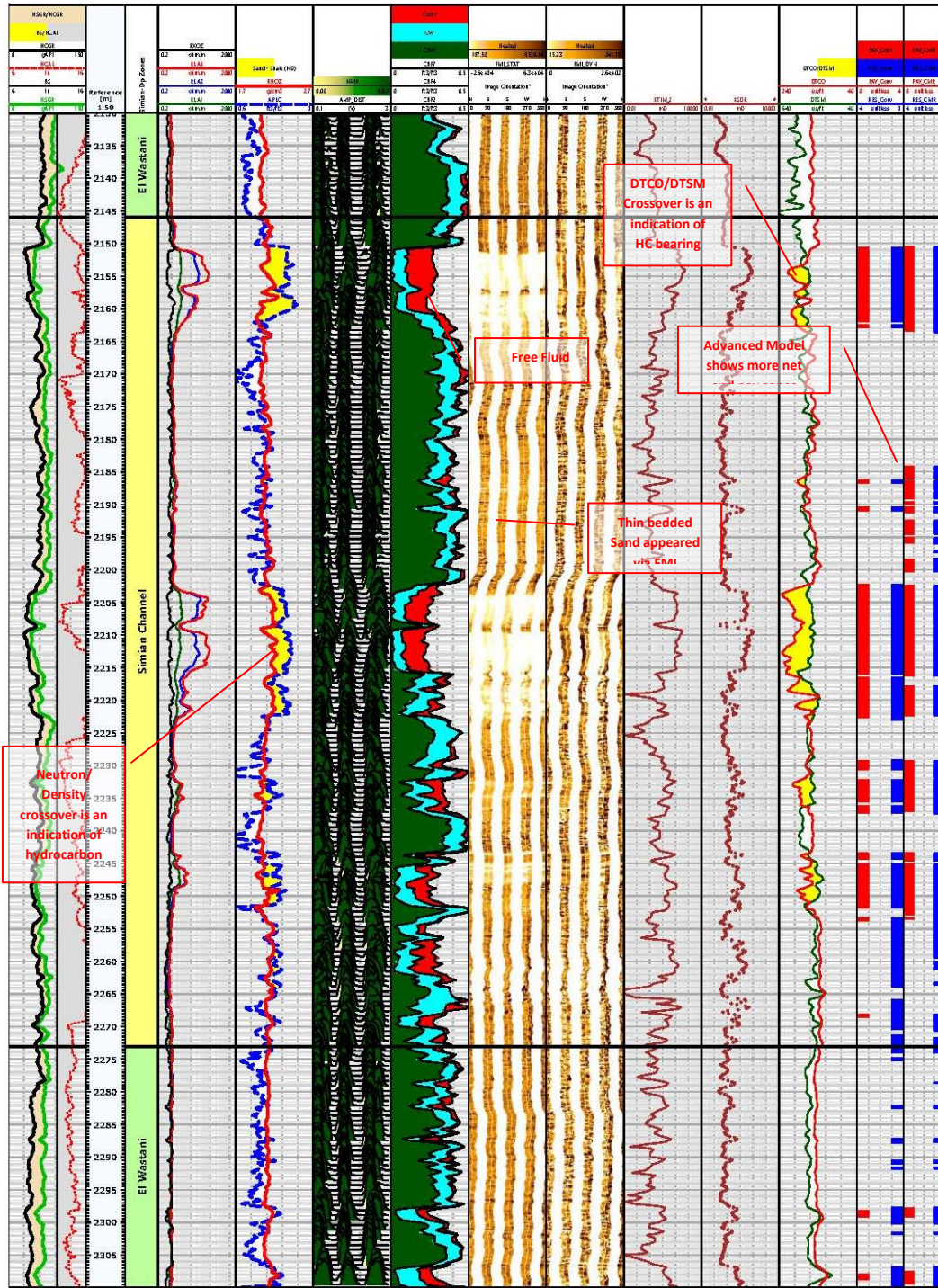


**Fig.6:** Litho-saturation plot showing integration of basic and advanced logs for detection of conventional and unconventional reservoirs for Simian Channel (El Wastani Formation) in Simian-Dp well

### 3.2. Reservoir Characterization (Simian Channel)

#### A) Histogram Charts for the Petrophysical Parameters

A histogram is the most used graph, to show the petrophysical parameters distributions. A property distribution shows how often each different value, in a set of data, occurs. Individual histograms of the equivalent petrophysical parameters calculated by conventional petrophysical model in each well were then compared to the advanced petrophysical histograms to determine the normalization shift. In general, a comparison of the conventional and the advanced calculated effective porosity, water saturation and volume of shale for the Simian channel showed a slight difference in the shape. Histogram bars refer to left axis (frequency) and cumulative frequency line (cumulative) refers to the right axis. (Fig. 7).

##### a. Effective Porosity Histogram

The average effective porosity (Fig. 7a) determined from the conventional model is 18% and the range is from 0 to 40%. The advanced petrophysical model is showing 20% average effective porosity with the range from 5 % to 35%.

##### b. Water Saturation Histogram

The calculated water saturation using the conventional petrophysical model ranged from 7% to 100%, with an average of 46% (Fig. 7b). Higher average water saturation 58% is observed from the advanced petrophysical read with the range from 6.5% to 100%.

##### c. Volume of Shale Histogram

The average volume of shale calculated using the conventional petrophysical model is 22%. The average shale volume has increased to 26% in the advanced petrophysical model. This is illustrated by the well shown in (Fig. 7c).

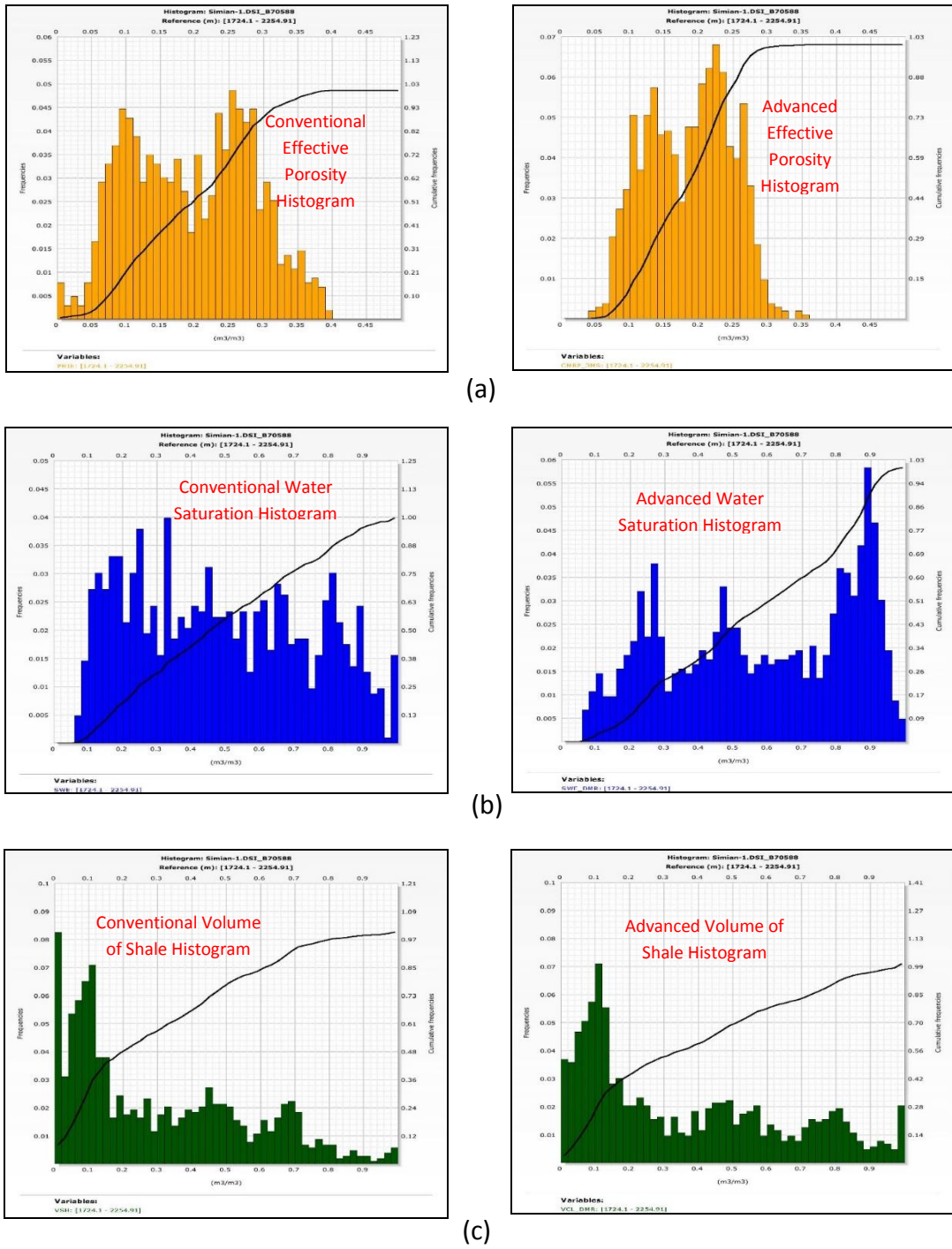


**Fig. 7:** Histogram charts showing a comparison between conventional and advanced calculated effective porosity, water saturation and volume of shale for Simian Channel (El Wastani Formation) in Simian-1 well

## **B) Distribution Maps for the Petrophysical Parameters**

### **a. Net-Pay Distribution Map**

The net-pay thickness distribution map of the Simian Channel (Fig. 8a) shows a considerable reservoir thickness, which is concentrated in the core of the channel, decreasing towards the edge, of the channel along its axis with a maximum recorded value of 60m by the conventional tools and 72m by the advanced methods of Simian-3 well. The thickness decreases gradually from central to both sides of the channel, recording the minimum reservoir thickness of 22m (conventional) and 31m (advanced) at Simian-2 well.

### **b. Effective Porosity Distribution Map**

The effective porosity distribution map of Simian Channel shows a very small variation in the porosity values (Fig. 8b), from a minimum value (21 %) at Simian-2 well to a maximum value (25 %) at Simian-3 well. This map shows an increase in the effective porosity at the core of the channel and to decrease along its axis of the channel.

### **c. Volume of Shale Distribution Map**

The volume of shale (Fig. 8c) shows variation in the shale content from a minimum value of (16 %) in Simian-1 well to a maximum value of (31 %) in Simian-2 well. Generally, the shale content distribution increases from core of the channel towards the channel axis.

### **d. Water Saturation Distribution Map**

The water saturation map of Simian Channel (Fig. 8d) shows variation in values, where minimum value of (29 %) of Simian-Dp well to a maximum of (38 %) of Simian-2 well. Generally, the water saturation distribution increases from the core of the channel toward the east of its edge along the axis.

### **e. Hydrocarbon Pore Volume Distribution Map**

The Hydrocarbon Pore Volume (HCP-V) map of (Fig. 8e) shows variation in the values, with the minimum value of (3.1 m) in Simian-2 well to a maximum value of (11.7 m) at Simian-3 well. Generally, the hydrocarbon pore volume (HCP-V) distribution decreases from the core of the channel towards the east of the edge of the channel along its axis.

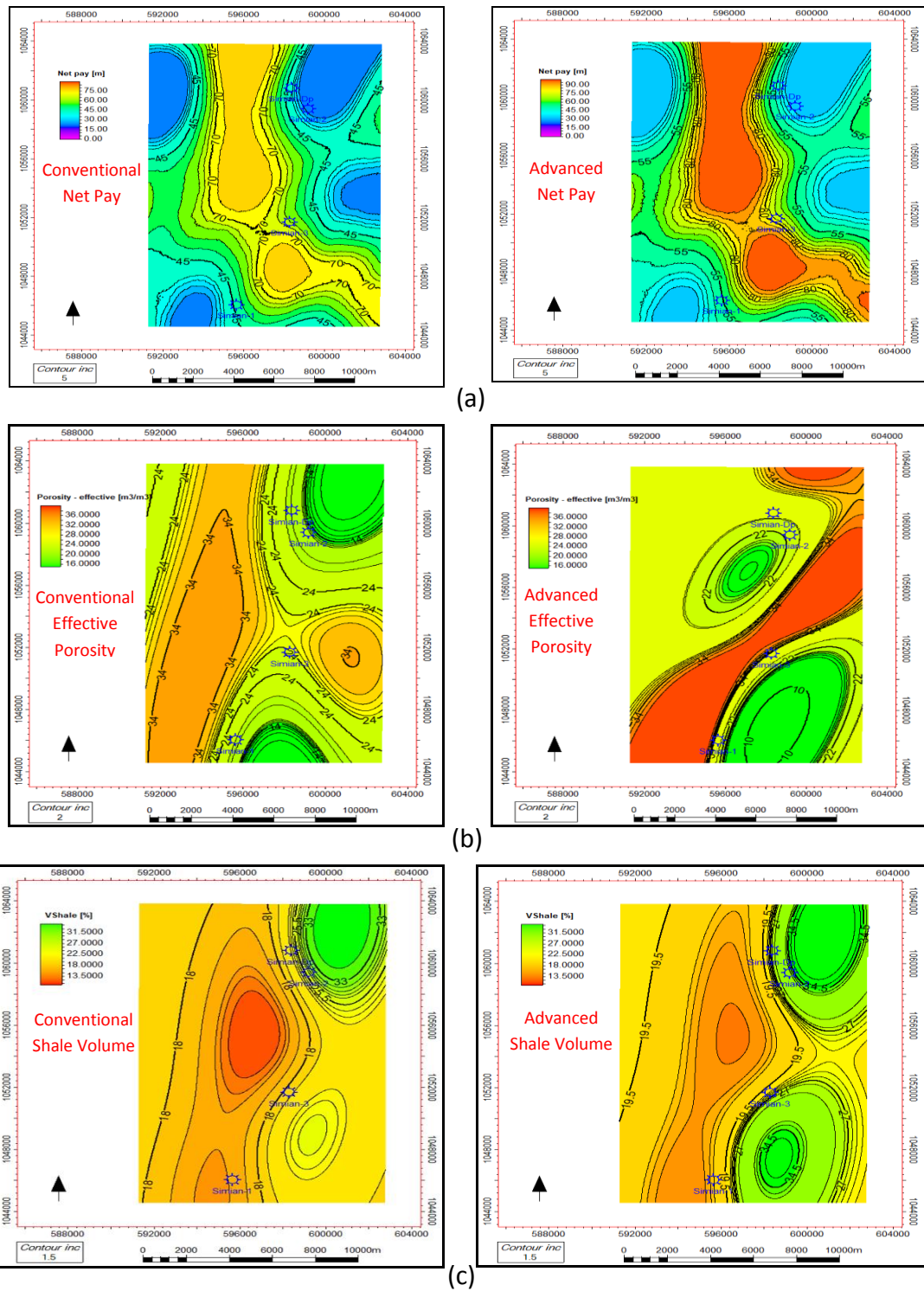


**Fig. 8:** Contour maps showing a comparison between conventional and advanced Net Pay (m), Effective Porosity (%), Shale Volume (%), Water Saturation (%) and HCP-V (m) for Simian Channel (El Wastani Formation) in Simian Field

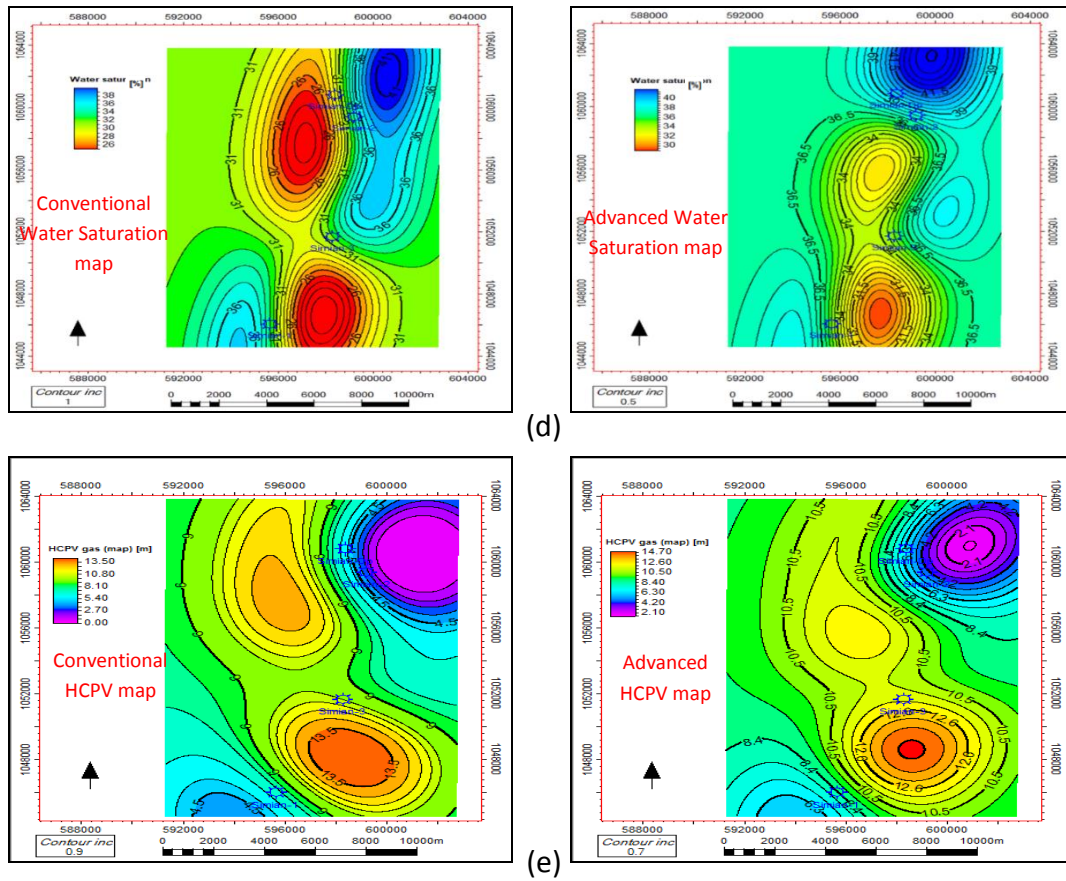


**Fig. 8:** (Continued) Contour maps showing a comparison between conventional and advanced Net Pay (m), Effective porosity (%), Shale Volume (%), Water Saturation (%) and HCP-V (m) for Simian Channel (El Wastani Formation) in Simian Field

## Conclusions

By making a combination of all the basic and advanced logging tools, the thin bedded sandstone reservoirs could be clearly detected and helped in adding new reserves to Simian Field that didn't appear before. This is through the detection of the amount of sands intercalated with shales and their hydrocarbon saturations. This new sand discovering increase the lifetime of production and to build understanding of the setting of Simian Field.

The results showed clean sandstone reservoirs and thin bedded sandstone through the use of advanced tools, which generally yielded an increase in the petrophysical parameters. The optimum location for the suggested new well is at the southeastern part of the field, which gave the best petrophysical parameters. It has high porosity, hydrocarbon saturation and net to gross thickness, in addition to low shale volume.

## REFERENCES

- Beshry, S., (2014).** "Reservoir Characterization of El Wastani Formation in Simian Channel, Simian Sienna Field, West Delta Deep Marine, Offshore Nile Delta, Egypt, MSC. thesis, Faculty of Science, Menoufiya University, Cairo. Egypt 27p".
- British Gas (BG). (1999).** "Final Well Report of Simian-1, Unpublished Internal Report".
- Coates, G.R., L.Z. Xiao, and M.G. Prammer (1999).** "NMR Logging – Principles and Applications, Gulf Publ. Co., Houston, 256 pp".
- Dewan, J. T. (1983).** Essentials of modern open-hole log interpretation. Penn Well Books, PennWell Publishing Company, Tulsa, Oklahoma, 361p.
- Kenyon, W.E. (1997).** "Petrophysical principles of applications of NMR logging, *The Log Analyst*, 38(2): 21-43.
- Rashpetco/BG (2005).** "Final Well Reports of Simian-Dp, Unpublished Internal Report".
- Schlumberger (1972).** The essential of log interpretation practice. Schlumberger Ltd., France, pp. 45-67.
- Schlumberger (1987).** "Log interpretation, Principles/Applications. Schlumberger Educational Service, Houston, Texas 77010, USA, 189p".
- Schlumberger (2004).** "Interactive Petrophysics software, operating manual, Version 3".
- Shehab, (2018).** "Reservoir Characterization and Hydrocarbon detection with conventional and advanced methods for Kafr El-Sheikh Formation at Sapphire Field, Offshore Nile Delta, Egypt 16p".
- Timur, A. (1968).** An investigation of permeability and porosity and residual water saturation relationships for sandstone reservoir. *The Log Analyst*, 9: 61.
- Wyllie, M.R.J. (1963).** The fundamentals of well log interpretation. New York Academic. Ed. 3, 1963. xvi + 238 pp.

## تقييم رسوبيات البلايوسين باستخدام الطرق البتروفيزيكية التقليدية والمتطورة لحقل بترول سيميان البحري (دلتا النيل البحري، مصر)

حسن القاضي، محمد مسعد ، أشرف السيد

قسم الجيولوجيا – كلية العلوم – جامعة الأزهر

### الخلاصة:

تقع منطقة الدراسة ١٢٠ كم شمال شرق مدينة الإسكندرية، حيث يقع هذا المنكون على عمق يتراوح بين (٢٥٠ – ١٥٠٠ م) من دلتا النيل، وتقع بين خطي عرض (١٦° ٣٢') و (٠٦° ٣٢') شمالاً وخطي طول (٤٤° ٣٠') و (٥٦° ٣٠') شرقاً. قناة سيميان هي واحدة من أنظمة القنوات الرئيسية التي تشكل مجمع القنوات العميقة منتصف العصر الحديث المعين في امتياز غرب الدلتا البحرية العميقة.

المواد المستخدمة في هذه الدراسة تشمل جمع ووصف وتحليل أربعة آبار. وكذلك مجموعات سجل كامل من أربعة آبار في منطقة الدراسة، وتشمل التالي: تسجيلات الآبار متمثلة في الأدوات الأساسية (أشعة جاما، مقياس قطر البئر، تسجيلات المقاومة الكهربية العميقة والضحلة) وأجهزة قياس المسامية (الكثافة والنيوترون والموجات الصوتية) وكذلك استخدام الأدوات متقدمة ذات دقة عالية مثل الصورة الدقيقة للمكون، والرنين المغناطيسي، والاختبار الديناميكي للضغط.

التفسيرات البتروفيزيكية أعطت ان متوسط المسامية الفعلية المحسوبة هو من ٢١٪ الى ٢٥٪ ومتوسط تشبع الصخر بالماء هو من ٢٩٪ الى ٤٠٪ ومتوسط حجم الصخر الطيني هو من ١٦٪ الى ٢٩٪. وفي العموم يستنتج ان توزيع الخصائص البتروفيزيكية هذه يزداد من وسط القناة الى الجوانب على طول القناة.

ولقد اظهرت النتائج ان المواقع المبشرة للآبار القادمة هو الجنوب الشرقي للحقل لأنه يحتوي على الخصائص البتروفيزيكية الافضل. فهي تحتوي على أعلى مسامية وتشبع الصخر بالنفط ونسبة حجم النفط الى حجم الصخر بالإضافة الى انها تحتوي على اقل نسبة للصخر الطيني. لكن يجب ان نأخذ في الاعتبار ان دمج الخرائط التركيبية والخرائط البتروفيزيكية ضروريا لتحديد الاماكن الافضل للآبار الجديدة في الاجزاء ذات الظواهر التركيبية المرتفعة والخصائص البتروفيزيكية الافضل.